doi: 10.15407/ujpe61.01.0066

I.V. BOYKO

I. Pulyui National Technical University of Ternopil
(56, Rus'ka Str., Ternopil 46001, Ukraine; e-mail: boyko.i.v.theory@gmail.com)

ROLE OF TWO-PHOTON ELECTRONIC TRANSITIONS IN THE FORMATION OF ACTIVE DYNAMIC CONDUCTIVITY IN A THREE-BARRIER RESONANCE TUNNELING STRUCTURE WITH AN APPLIED DC ELECTRIC FIELD

PACS 73.21.Fg, 73.40.Gk, 73.63.Hs

The theory of active dynamic conductivity in a three-barrier resonance tunneling structure subjected to the combined action of a weak electromagnetic field and a longitudinal dc electric field is developed with regard for the contribution of laser-induced one- and two-photon electronic transitions with different frequencies. For this purpose, the full Schrödinger equation is solved in the effective mass approximation and with the use of the model of rectangular potential wells and barriers for an electron. The maximum contribution of two-photon transitions to the formation of the total active dynamic conductivity in laser-induced transitions is shown not to exceed 38%. Geometric configurations of the resonance tunneling structure, for which the laser radiation intensity increases due to laser-induced two-photon electronic transitions, are determined.

Keywords: resonance tunneling structure, quantum cascade laser, quantum cascade detector, active dynamic conductivity, two-photon electronic transition.

1. Introduction

The development of modern nanotechnologies, in which quantum cascade lasers (QCLs) [1,2] and quantum cascade detectors (QCDs) [3, 4] are applied, is inseparably connected with the research of transport properties of multilayered planar semiconductor resonance tunneling structures (RTSs) and physical processes in them. The choice of the geometrical design for RTSs, which are active elements of QCL and QCD cascades, and the application of a longitudinal dc electric field (in the case of QCLs) not only determine the operation frequency (energy) of those nanodevices, but also provides an efficient coordinated work of nanodevice cascades.

As was shown in works [5–7], the consideration of RTSs as open nanosystems and the research of the physical processes responsible for the amplification of active current (this phenomenon is associated with the active dynamic conductivity that arises in RTSs in an electromagnetic field owing to quantum transitions occurring between electron states and accompanied by the emission or absorption of electromagnetic waves) provide an effective method to optimize the operational parameters of QCLs and QCDs. One of the ways to enhance the output RTS current is the photon-assisted tunneling in a strong electromagnetic field [8, 9], when new non-resonance channels of nanostructure transparency emerge [10, 11]. The case of two-photon quantum transitions between quasi-stationary electronic states with the emission of photons with identical or different frequencies was studied in works [12, 13] in the framework of rough models: δ-like potential barriers in RTSs and a common effective electron mass.

In this connection, the main results obtained in the cited works have only a qualitative character and, as is known [14], cannot be applied to optimize the geometrical design of the active zone or cascade in QCLs and QCDs. A required theory has to be based on a more realistic model, e.g., rectangular potentials and different effective electron masses in different media of the open nano-RTS. In this case, such an essential factor as finite electron lifetimes in quasi-stationary states, which, to some extent, determines the dynamic conductivity and is one of the factors that make the optimization of

© I.V. BOYKO, 2016

a nanodevice operation possible, can be taken into account.

In this work, a quantum-mechanical theory of active dynamic conductivity in a three-barrier active zone of QCL with one- and two-photon electronic transitions characterized by different frequencies is developed in the framework of the models of effective electron masses and rectangular potential wells and barriers, by applying the perturbation theory in the framework of the weak-signal approximation. Using the experimentally studied three-barrier RTS playing the role of active zone in a QCL with GaAs potential wells and $Al_xGa_{1-x}As$ potential barriers as an example, the dependence of the spectral characteristics of electronic quasi-stationary states and the dynamic conductivity formed by one- and two-photon quantum transitions of electrons accompanied by the electromagnetic wave emission on the geometric design of a structure is analyzed. Geometric configurations of three-barrier RTS, in which the conditions for a two-photon laser generation with the enhancement of the QCL radiation intensity to 38% can be realized, are found.

2. Theory of Active Dynamic Conductivity in the Three-Barrier Active Zone of a Quantum Cascade Laser in the Case of Two-Photon Electronic Transition

Let us consider a three-barrier RTS, which is so arranged in the Cartesian coordinate frame that the axis OZ is perpendicular to the medium interfaces in the nanosystem (Fig. 1). A dc electric field with the strength **F** is applied perpendicularly to the RTS layers. Taking into account an insignificant difference between the lattice constants in the well and barrier layers, the model of effective masses for the electron and the model of rectangular potentials are applied:

$$m(z) = m_0 \sum_{p=0}^{3} [\theta(z - z_{2p-1}) - \theta(z - z_{2p})] + \\ + m_1 \sum_{p=0}^{2} [\theta(z - z_{2p}) - \theta(z - z_{2p+1})], \quad (1)$$

$$U(z) = U_0 \sum_{p=0}^{2} [(\theta(z - z_{2p}) - \theta(z - z_{2p+1})] - \\ - eF \{z [\theta(z) - \theta(z - z_5)] + z_5 \theta(z - z_5)\}, \quad (2)$$

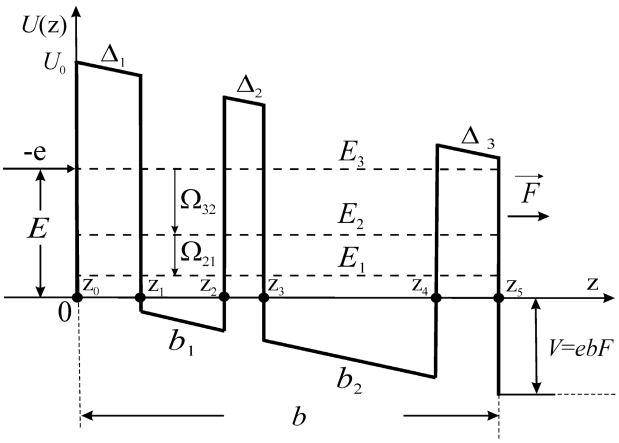

Fig. 1. Geometric and energy diagrams of a three-barrier RTS

where $\theta(z)$ is the Heaviside unit function, $z_{-1} \to -\infty$, $z_6 \to \infty$, and m_0 and m_1 are the effective electron masses in the RTS potential wells and barriers, respectively. Expression (2) for $U(z)$ describes the potential energy of an electron in the RTS with regard for the influence of a dc electric field, and U_0 in this expression is the value of electron energy in the absence of this field.

Let a monoenergetic flux of electrons with energy E close to the energy of the third energy level, $E \approx E_3$, and the concentration n_0 propagate from left to right along the axis OZ perpendicularly to the layers of three-barrier RTS. Under those conditions, the electron wave function $\Psi(z,t)$ has to satisfy the full Schrödinger equation:

$$i\hbar \frac{\partial \Psi(z,t)}{\partial t} = [H_0(z) + H(z,t)]\, \Psi(z,t), \quad (3)$$

where

$$H_0(z) = \frac{\hbar^2}{2} \frac{\partial}{\partial z} \frac{1}{m(z)} \frac{\partial}{\partial z} + U(z) \quad (4)$$

is the Hamiltonian of the corresponding stationary problem for the electron, and

$$H(z,t) = -e\Big[\mathcal{E}_1(e^{i\omega_1 t} + e^{-i\omega_1 t}) + \\ + \mathcal{E}_2(e^{i\omega_2 t} + e^{-i\omega_2 t})\, [z\theta(z) + (z_5 - z)\theta(z - z_5)]\Big] \quad (5)$$

is the Hamiltonian describing the interaction of electrons with a weak two-frequency electromagnetic field in the dipole approximation. The components of this

field are characterized by the frequencies ω_1 and ω_2, and the electric strength amplitudes $\mathcal{E}_1$ and $\mathcal{E}_2$, respectively.

In the weak-signal approximation and provided the two-photon transitions between electronic states, which are accompanied by the radiation and the absorption of electromagnetic waves, the solution of the Schrödinger equation (3) is sought in the second order of perturbation theory in the form

$$\Psi(z,t) = \Psi_0(z)e^{-i\omega_0 t} + \\ + \Psi_{-1}(z)e^{-i(\omega_0-\omega_1)t} + \Psi_{+1}(z)e^{-i(\omega_0+\omega_1)t} + \\ + \Psi_{-2}(z)e^{-i(\omega_0-\omega_1-\omega_2)t} + \Psi_{+2}(z)e^{-i(\omega_0+\omega_1+\omega_2)t}, \quad (6)$$

where $\omega_0 = E/\hbar$. Substituting Eq. (6) into Eq. (3), we obtain a system of equations for the wave function $\Psi_0(z)$ and the corresponding corrections of the first, $\Psi_{\pm1}(z)$, and second, $\Psi_{\pm2}(z)$, orders:

$$[H_0(z) - E]\,\Psi_0(z) = 0, \quad (7)$$

$$[H_0(z) - (E \pm \Omega_1)]\,\Psi_{\pm1}(z) - \\ - e\mathcal{E}_1\,[z\theta(z) + (z_5 - z)\theta(z - z_5)]\,\Psi_0(z) = 0, \quad (8)$$

$$[H_0(z) - (E \pm (\Omega_1 + \Omega_2)]\,\Psi_{\pm2}(z) - \\ - e\mathcal{E}_2\,[z\theta(z) + (z_5 - z)\theta(z - z_5)]\,\Psi_{\pm1}(z) = 0, \quad (9)$$

where $\Omega_1 = \hbar\omega_1$ and $\Omega_2 = \hbar\omega_2$. The solution of the stationary Schrödinger equation (7) is well known for each RTS region [5, 6]. Therefore, the function $\Psi_0(E,z)$ can be written in the form

$$\Psi_0(E,z) = \Psi_0^{(0)}(E,z)\theta(-z) + \Psi_0^{(6)}(E,z)\theta(z-z_5) + \\ + \sum_{p=1}^{5}\Psi_{E,0}^{(p)}(z)\,[\theta(z-z_{p-1}) - \theta(z-z_p)] = \\ = (A_0^{(0)}e^{ik_0^{(0)}z} + B_0^{(0)}e^{-ik_0^{(0)}z})\theta(-z) + \\ + A_0^{(6)}e^{ik_0^{(6)}(z-z_5)}\theta(z-z_5) + \\ + \sum_{p=1}^{5}\left[A_0^{(p)}Ai(\xi^{(p)}(z)) + B_0^{(p)}Bi(\xi^{(p)}(z))\right] \times \\ \times\,[\theta(z-z_{p-1}) - \theta(z-z_p)], \quad (10)$$

where $A_0^{(0)}$ and $B_0^{(0)}$ are coefficients in the solution of Eq. (7) to the left from the RTS, $B_0^{(6)}$ to the right from the RTS, and $A_0^{(p)}$ and $B_0^{(p)}$ in the RTS, $Ai(\xi)$ and $Bi(\xi)$ are the Airy functions,

$$k_0^{(0)} = \hbar^{-1}\sqrt{2m_0E}, \quad k_0^{(6)} = \hbar^{-1}\sqrt{2m_0(E+eFz_5)},$$

$$\xi^{(1)}(z) = \xi^{(3)}(z) = \xi^{(5)}(z) = \\ = \left(2m_1eF/\hbar^2\right)^{1/3[(U_0-E)/eF-z]}, \quad (11)$$

$$\xi^{(2)}(z) = \xi^{(4)}(z) = -\left(2m_0eF/\hbar^2\right)^{1/3}[E/eF + z].$$

The wave function $\Psi_0(E,z)$ determined according to relations (10) satisfies the normalization condition

$$\int_{-\infty}^{\infty}\Psi_0^*(k',z)\Psi_0(k,z)dz = \delta(k-k') \quad (12)$$

and allows us to calculate the distribution function for the density of probability to find an electron in the RTS analytically:

$$W(E,z) = \frac{1}{z_5}\int_0^{z_5}|\Psi_0(E,z)|^2\,dz. \quad (13)$$

This function determines the spectral characteristics of quasi-stationary electronic states: the resonance energies E_n and the lifetimes τ_n [14].

In view of the analytical complexity of Eqs. (8) and (9), it is expedient to solve them, by using the linear approximation for the effective potential $U_{\text{eff}}(z) = \\ = U(z)$ in each RTS layer (see, e.g., work [15]). Then the approximate effective potential for an electron looks like

$$\tilde{U}_{\text{eff}}(z) = \sum_{p=1}^{5}\sum_{l=0}^{N}U(z_{p_l})[\theta(z-z_{p_l}) - \theta(z-z_{p_{l+1}})], \quad (14)$$

where

$$z_{p_l} = \frac{l}{2N}(z_p - z_{p-1}), \quad p = 1\div5; \quad z_0 = 0, \quad (15)$$

and N is the number of mesh intervals in the p-th RTS layer. Now, the solution of the stationary Schrödinger equation (7) can be written with a required accuracy in the form

$$\Psi_0(E,z) = \Psi_0^{(0)}(z)\theta(-z) + \Psi_0^{(6)}(z)\theta(z-z_5) + \\ + \sum_{p=1}^{5}\sum_{l=0}^{N}\Psi_{0l}^{(p)}(z)\left[\theta(z-z_{p_l}) - \theta(z-z_{p_{l+1}})\right] =$$

$$= (A_0^{(0)} e^{ik_0^{(0)} z} + B_0^{(0)} e^{-ik_0^{(0)} z})\theta(-z) +$$
$$+ A_0^{(6)} e^{ik_0^{(6)}(z-z_5)}\theta(z-z_5) +$$
$$+ \sum_{p=1}^{5}\sum_{l=0}^{N}[A_{0l}^{(p)} e^{ik_0^{(p_l)}(z-z_{p_l})} + B_{0l}^{(p)} e^{-ik_0^{(p_l)}(z-z_{p_l})}] \times$$
$$\times \left[\theta(z-z_{p_l}) - \theta(z-z_{p_{l+1}})\right], \quad (16)$$

where

$$k_0^{(p_l)} = \begin{cases} \hbar^{-1}\sqrt{2m_0(E+eFz_{p_l})}, \\ z_{p_l} \in (z_1,\, z_2)\bigcup(z_3,\, z_4); \\ \hbar^{-1}\sqrt{2m_1(E-U_0+eFz_{p_l})}, \\ z_{p_l} \in (z_0,\, z_1)\bigcup(z_2,\, z_3)\bigcup(z_4,\, z_5), \end{cases} \quad (17)$$

and $A_{0l}^{(p)}$ and $B_{0l}^{(p)}$ are coefficients in the solutions of Eq. (7) for the l-th interval in the p-th RTS layer. Those coefficients, as well as the coefficients $A_0^{(p)}$ and $B_0^{(p)}$, are determined from the continuity conditions for the wave function $\Psi_0(E,z)$ and the fluxes of probability density across the heterointerfaces between all layers in the nanostructure and across the boundaries of mesh intervals created, while approximating the effective potential.

The required accuracy of solutions (16), which was mentioned above, is determined by the evident condition

$$\varepsilon = \frac{\left|\left|\Psi_0(E,z)\right|^2 - \left|\tilde{\Psi}_0(E,z)\right|^2\right|}{\left|\Psi_0(E,z)\right|^2} \ll 1, \quad (18)$$

where $\Psi_0(E,z)$ and $\tilde{\Psi}_0(E,z)$ are solutions (10) and (16), respectively.

The solutions of Eqs. (8) and (9) are superpositions of two functions:

$$\Psi_{\pm\alpha}(z) = \psi_{\pm\alpha}(z) + \Phi_{\pm\alpha}(z) \quad (\alpha = 1,\, 2). \quad (19)$$

The functions

$$\psi_{\pm\alpha}(z) = \psi_{\pm\alpha}^{(0)}(z)\theta(-z) + \psi_{\pm\alpha}^{(6)}(z)\theta(z-z_5) +$$
$$+ \sum_{p=1}^{5}\sum_{l=0}^{N}\psi_{\pm\alpha l}^{(p)}(z)\left[\theta(z-z_{p_l}) - \theta(z-z_{p_{l+1}})\right] =$$
$$= B_{\pm\alpha}^{(0)} e^{-ik_{\pm\alpha}^{(0)} z}\theta(-z) + A_{\pm\alpha}^{(6)} e^{ik_{\pm\alpha}^{(6)}(z-z_5)}\theta(z-z_5) +$$
$$+ \sum_{p=1}^{5}\sum_{l=0}^{N}\left[A_{\pm\alpha l}^{(p)} e^{ik_{\pm\alpha}^{(p_l)}(z-z_{l-1})} + B_{\pm\alpha l}^{(p)} e^{-ik_{\pm\alpha}^{(p_l)}(z-z_{l-1})}\right] \times$$
$$\times \left[\theta(z-z_{p_l}) - \theta(z-z_{p_{l+1}})\right] \quad (20)$$

are solutions of the homogeneous equations (8) and (9). The signs "+" and "−" correspond to the processes associated with the emission and the absorption of an electromagnetic field, respectively. The functions

$$\Phi_{\pm1}(z) = \sum_{p=1}^{5}\sum_{l=0}^{N}\Phi_{\pm1l}^{(p)}(z)\left[\theta(z-z_{p_l}) - \theta(z-z_{p_{l+1}})\right] +$$
$$+ \Phi_{\pm1}^{(6)}(z)\theta(z-z_5) =$$
$$= \sum_{p=1}^{5}\sum_{l=0}^{N}\left[\mp\frac{U_1}{\Omega_1}\frac{z}{z_5}\Psi_{0l}^{(p)}(z) + \frac{\hbar^2 U_1}{m_l z_5 \Omega_1^2}\frac{d\Psi_{0l}^{(p)}(z)}{dz}\right] \times$$
$$\times \left[\theta(z-z_{p_l}) - \theta(z-z_{p_{l+1}})\right] \mp \frac{U_1}{\Omega_1}\Psi_0^{(6)}(z)\theta(z-z_5), \quad (21)$$

and

$$\Phi_{\pm2}(z) = \sum_{p=1}^{5}\sum_{l=0}^{N}\Phi_{\pm2l}^{(p)}(z)\left[\theta(z-z_{p_l}) - \theta(z-z_{p_{l+1}})\right] +$$
$$+ \Phi_{\pm2}^{(6)}(z)\theta(z-z_5) =$$
$$= \sum_{p=1}^{5}\sum_{l=0}^{N}\Bigg[\frac{U_1 U_2}{\Omega_1(\Omega_1+\Omega_2)}\left(\frac{\hbar^2}{m_{p_l} z_5^2}\frac{\Omega_1+\Omega_2 \mp 4E_0}{(\Omega_1+\Omega_2)^2} +\right.$$
$$\left. + \left(\frac{z}{z_5}\right)^2\right)\Psi_{0l}^{(p)}(z) + \left(\frac{\hbar^2\sqrt{U_1 U_2}}{m_{p_l} z_5 \Omega_1(\Omega_1+\Omega_2)}\right)^2 \frac{d^2\Psi_{0l}^{(p)}(z)}{dz^2} \mp$$
$$\mp \frac{\hbar^2}{m_{p_l} z_5^2}\frac{U_1 U_2(3\Omega_1+\Omega_2)}{\Omega_1^2(\Omega_1+\Omega_2)^2} z\frac{d\Psi_{0l}^{(p)}(z)}{dz} \mp$$
$$\mp \frac{U_2}{\Omega_2}\frac{z}{z_5}\psi_{\pm1l}^{(p)}(z) + \frac{\hbar^2 U_2}{m_{p_l} z_5 \Omega_2^2}\frac{d\psi_{\pm1l}^{(p)}(z)}{dz}\Bigg] \times$$
$$\times \left[(z-z_{p_l}) - \theta(z-z_{p_{l+1}})\right] +$$
$$+ \left(\frac{U_1 U_2}{\Omega_1(\Omega_1+\Omega_2)}\Psi_0^{(6)}(z) \mp \frac{U_2}{\Omega_2}\psi_{\pm1}^{(6)}(z)\right)\theta(z-z_5) \quad (22)$$

are solutions of the inhomogeneous equations (8) and (9). Here,

$$U_1 = e\mathcal{E}_1 z_5, U_2 = e\mathcal{E}_2 z_5,$$

$$m_{p_l} = \begin{cases} m_0, & z_{p_l} \in (z_1,\, z_2)\bigcup(z_3,\, z_4); \\ m_1, & z_{p_l} \in (z_0,\, z_1)\bigcup(z_2,\, z_3)\bigcup(z_4,\, z_5), \end{cases} \quad (23)$$

$$k_{\pm1}^{(p_l)} = \begin{cases} \hbar^{-1}\sqrt{2m_0(E+eFz_{p_l}\pm\Omega_1)}, \\ z_{p_l} \in (z_1,\, z_2)\bigcup(z_3,\, z_4); \\ \hbar^{-1}\sqrt{2m_1(E-U_0+eFz_{p_l}\pm\Omega_1)}, \\ z_{p_l} \in (z_0,\, z_1)\bigcup(z_2,\, z_3)\bigcup(z_4,\, z_5), \end{cases} \quad (24)$$

$$k_{\pm 2}^{(p_l)} = \begin{cases} \hbar^{-1}\sqrt{2m_0(E + eFz_{p_l} \pm (\Omega_1 + \Omega_2))}, \\ z_{p_l} \in (z_1,\, z_2) \bigcup (z_3,\, z_4); \\ \hbar^{-1}\sqrt{2m_1(E - U_0 + eFz_{p_l} \pm (\Omega_1 + \Omega_2))}, \\ z_{p_l} \in (z_0,\, z_1) \bigcup (z_2,\, z_3) \bigcup (z_4,\, z_5). \end{cases} \tag{25}$$

All unknown coefficients – these are $A_0^{(0)}$, $B_0^{(0)}$, $A_0^{(6)}$, $A_{0l}^{(p)}$, $B_{0l}^{(p)}$, $B_{\pm 1}^{(0)}$, $A_{\pm 1}^{(6)}$, $A_{\pm 1l}^{(p)}$, $B_{\pm 1l}^{(p)}$, $B_{\pm 2}^{(0)}$, $A_{\pm 2}^{(6)}$, $A_{\pm 2l}^{(p)}$, and $B_{\pm 2l}^{(p)}$ ($p = 0 \div 5$, $l = 0 \div N$) – are unambiguously found from the continuity conditions for the wave function $\Psi(z,t)$ and the probability density fluxes across all RTS heterointerfaces at an arbitrary time moment t,

$$\Psi^{(p_l)}(z_{p_l}, t) = \Psi^{(p_{l+1})}(z_{p_l}, t);$$

$$\frac{1}{m_{p_l}} \frac{d\Psi^{(p_l)}(z,t)}{dz}\bigg|_{z=z_{p_l}} = \frac{1}{m_{p_{l+1}}} \frac{d\Psi^{(p_{l+1})}(z,t)}{dz}\bigg|_{z=z_{p_l}}, \tag{26}$$

which together with normalization condition (12) unambiguously determine the wave function $\Psi_0(z)$, the corrections $\Psi_{\pm 1}(z)$ and $\Psi_{\pm 2}(z)$ to it, and, hence, the total wave function $\Psi(z,t)$.

After analytically calculating the energy of interaction between the electron and the electromagnetic field as a sum of the energies of the electron waves emitted from the both sides of nano-RTS, we can find, in the quasi-classical approximation, a formula for the real part of the active conductivity σ in terms of the flux densities of those waves [5–7]:

$$\begin{aligned} \sigma^{(\mathrm{II})}(\Omega_1, \Omega_2, E) = {} & \frac{\Omega_1}{2z_5 e\mathcal{E}_1^2}\{[j_{+1}(E + \Omega_1, z = z_5) - \\ & - j_{-1}(E - \Omega_1, z = z_5)] - [j_{+1}(E + \Omega_1, z = z_0) - \\ & - j_{-1}(E - \Omega_1, z = z_0)]\} + \\ & + \frac{(\Omega_1 + \Omega_2)}{2z_5 e\mathcal{E}_2^2}\{[j_{+2}(E + \Omega_1 + \Omega_2, z = z_5) - \\ & - j_{-2}(E - (\Omega_1 + \Omega_2), z = z_5)] - \\ & - [j_{+2}(E + \Omega_1 + \Omega_2, z = z_0) - \\ & - j_{-2}(E - (\Omega_1 + \Omega_2),\, z = z_0)]\}, \end{aligned} \tag{27}$$

where the first four terms describe the densities of electron fluxes that arise in one-photon electron transitions, and the following four terms in two-photon ones.

According to quantum mechanics, the densities of electron currents that arise in the RTS as a result of the quantum transitions between the electronic states with the energy emission or absorption in one-, $\Psi_{\pm 1}(z)$, and two-photon, $\Psi_{\pm 2}(z)$, transitions are determined by the expression

$$\begin{aligned} j_{\pm\alpha}(E,z) = {} & \frac{ie\hbar n_0}{2m_0}\left(\Psi_{\pm\alpha}(E,z)\frac{d\Psi^*_{\pm\alpha}(E,z)}{dz} - \right. \\ & \left. - \Psi^*_{\pm\alpha}(E,z)\frac{d\Psi_{\pm\alpha}(E,z)}{dz}\right), \quad \alpha = 1,\ 2. \end{aligned} \tag{28}$$

In view of Eq. (29), the real part of the dynamic RTS conductivity σ is taken as a sum of two partial components,

$$\sigma^{(\mathrm{II})}(\Omega_1,\ \Omega_2) = \sigma^{(1)}(\Omega_1) + \sigma^{(2)}(\Omega_1,\ \Omega_2), \tag{29}$$

where

$$\sigma^{(1)}(\Omega_1) = \sigma^{(1)+}(\Omega_1) + \sigma^{(1)-}(\Omega_1) \tag{30}$$

is the conductivity in the first order of perturbation theory (i.e. formed by one-photon electronic transitions) and

$$\sigma^{(2)}(\Omega_1,\ \Omega_2) = \sigma^{(2)+}(\Omega_1,\ \Omega_2) + \sigma^{(2)-}(\Omega_1,\ \Omega_2) \tag{31}$$

is the conductivity in the second order of perturbation theory (i.e. formed by two-photon electronic transitions). Here,

$$\begin{aligned} \sigma^{(1)+}(\Omega_1) = {} & \frac{e^2\hbar\,\Omega_1 z_5 n_0}{2m_0 U_1^2}\left(k_{+1}^{(6)}\left|A_{+1}^{(6)}\right|^2 - \right. \\ & \left. - k_{-1}^{(6)}\left|A_{-1}^{(6)}\right|^2 + \frac{U_1}{2\Omega_1}\left(P_{01}^{+} - P_{01}^{-}\right)\right), \end{aligned} \tag{32}$$

$$\sigma^{(1)-}(\Omega_1) = \frac{e^2\hbar\,\Omega_1 z_5 n_0}{2m_0 U_1^2}\left(k_{+1}^{(0)}\left|B_{+1}^{(0)}\right|^2 - k_{-1}^{(0)}\left|B_{-1}^{(0)}\right|^2\right), \tag{33}$$

$$\begin{aligned} \sigma^{(2)+}(\Omega_1,\ \Omega_2) = {} & \frac{e^2\hbar(\Omega_1 + \Omega_2)\, z_5 n_0}{m_0 U_2^2} \times \\ & \times \left(\frac{U_2}{2\Omega_2}\left(P_{12}^{+} - P_{12}^{-}\right) + k_{+2}^{(6)}\left|A_{+2}^{(6)}\right|^2 - k_{-2}^{(6)}\left|A_{-2}^{(6)}\right|^2 + \right. \\ & + \frac{U_1 U_2}{2\Omega_1\,(\Omega_1 + \Omega_2)}\left(P_{02}^{+} - P_{02}^{-}\right) + \\ & + \left(\frac{U_2}{\Omega_2}\right)^2\left(k_{+1}^{(6)}\left|A_{+1}^{(6)}\right|^2 - k_{-1}^{(6)}\left|A_{-1}^{(6)}\right|^2\right) + \\ & \left. + \frac{U_1\, U_2^2}{2\Omega_1\,\Omega_2(\Omega_1 + \Omega_2)}\left(P_{01}^{+} - P_{01}^{-}\right)\right), \end{aligned} \tag{34}$$

$$\sigma^{(2)-}(\Omega_1,\ \Omega_2) = \frac{e^2\hbar(\Omega_1+\Omega_2)\, z_5 n_0}{m_0 U_2^2} \times$$

$$\times \left(k_{+2}^{(0)} \left|B_{+2}^{(0)}\right|^2 - k_{-2}^{(0)} \left|B_{-2}^{(0)}\right|^2\right), \qquad (35)$$

$$P_{01}^{\pm} = \mp(k_0^{(6)} + k_{\pm1}^{(6)}) \left(A_0^{(6)} A_{\pm1}^{(6)*} + A_0^{(6)*} A_{\pm1}^{(6)}\right), \qquad (36)$$

$$P_{02}^{\pm} = (k_0^{(6)} + k_{\pm2}^{(6)}) \left(A_0^{(6)} A_{\pm2}^{(6)*} + A_0^{(6)*} A_{\pm2}^{(6)}\right), \qquad (37)$$

$$P_{12}^{\pm} = \mp(k_{\pm1}^{(6)} + k_{\pm2}^{(6)}) \left(A_{\pm1}^{(6)} A_{\pm2}^{(6)*} + A_{\pm1}^{(6)*} A_{\pm2}^{(6)}\right). \qquad (38)$$

The introduced partial components $\sigma^+(\Omega)$ and $\sigma^-(\Omega)$ correspond to the conductivities of the electron fluxes directed to the output and the input of RTS, respectively, relatively to the direction of the initial electron flux.

Note that, as one can see from relations (21), (32), (33), and (36) ($A_{\pm1}^{(6)}, A_{\pm1}^{(6)*}, B_{\pm1}^{(6)}, P_{01}^{\mp} \sim U_1$), the dynamic conductivity does not depend on the strength of electric components of the electromagnetic field in the first order of perturbation theory [5–7]. At the same time, as one can see from formulas (22), (34), (35), (37), and (38) ($A_{\pm2}^{(6)}$, $A_{\pm2}^{(6)*}, B_{\pm2}^{(6)}, P_{02}^{\mp} \sim U_1U_2$ and $P_{12}^{\mp} \sim U_1^2U_2$), the dynamic conductivity found in the second order of perturbation theory, on the contrary, turns out dependent on the strengths of electric components of the electromagnetic field.

3. Discussion

It is clear from physical considerations that the optimal performance of a QCL with an arbitrary geometrical design of its active zone depends on whether the maximum of the dynamic conductivity $\sigma^+(\Omega)$ formed by a direct electron flow is attained in the required frequency interval or not. The approach to the optimization of the work of cascade nanodevices operating in the single-mode regime, which was developed in works [5–7], can be generalized to the case of optimization of the geometrical design of the QCL active zone for the processes of two-photon generation.

Specific calculations were carried out for an experimentally researched three-barrier RTS [16] with GaAs potential wells and $Al_{0.15}Ga_{0.85}As$ potential barriers, which is characterized by the following known physical parameters: $n_0 = 3.2 \times 10^{15}$ cm^{-3}, $m_0 = 0.063m_e$, where m_e is the free electron mass, $m_1 = 0.075m_e$, $U = 516$ meV, and $F = 17$ kV/cm. The geometrical parameters of the examined three-barrier

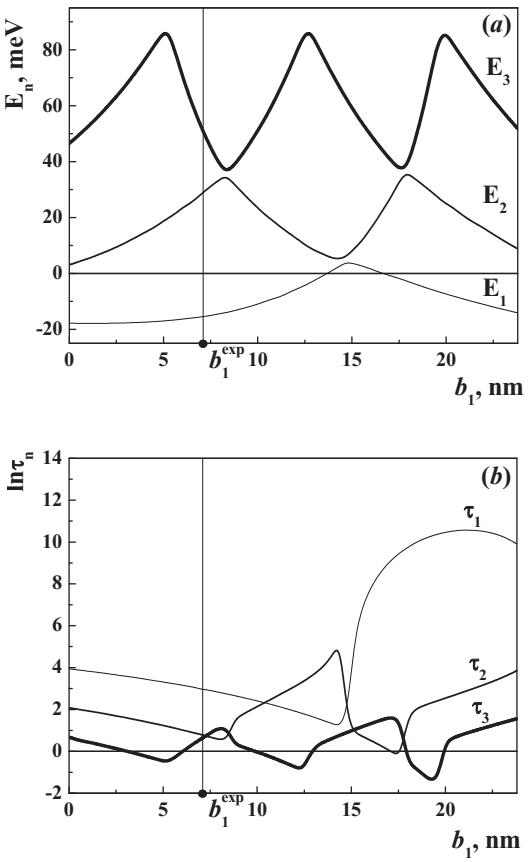

Fig. 2. Dependences of the electron resonance energies E_n (a) and the lifetimes τ_n in picosecond units (b) on the position b_1 of the internal barrier in a common potential well

RTS are as follows: the widths of the potential wells $b_1 = 7.1$ nm and $b_2 = 16.7$ nm; and the thicknesses of the input, internal, and output potential barriers $\Delta_1 = 5.6$ nm, $\Delta_2 = 3.1$ nm, and $\Delta_3 = 5.6$ nm, respectively. The results of calculations of the resonance energies (E_1, E_2, and E_3) and the lifetimes (τ_1, τ_2, and τ_3) of the first three quasi-stationary electron states as functions of the internal barrier position b_1 in the common potential well b, when the other geometrical parameters of RTS are fixed, are depicted in Fig. 2.

The energies of quantum transitions $\Omega_{32}^{\text{theor}} = E_3 - E_2 = 20.8$ meV and $\Omega_{21}^{\text{theor}} = E_2 - E_1 = 41.1$ meV, which are theoretically calculated in this work for the experimentally realized geometrical configuration of RTS (b_1^{exp}), differ from the experimental values $\Omega_{32}^{\text{exp}} = 19$ meV and $\Omega_{21}^{\text{exp}} = 37$ meV obtained in work [16] by no more than 10%. The lifetimes of an electron in the first three working quasi-stationary

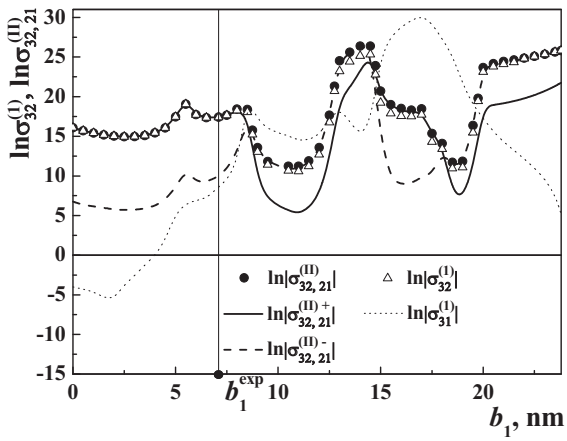

Fig. 3. Dependences of the dynamic conductivity (in S/cm units) formed in the one-, $\sigma^{(1)}$, and two-photon, $\sigma^{(II)}$, quantum laser transitions on the position b_1 of the internal barrier in a common potential well

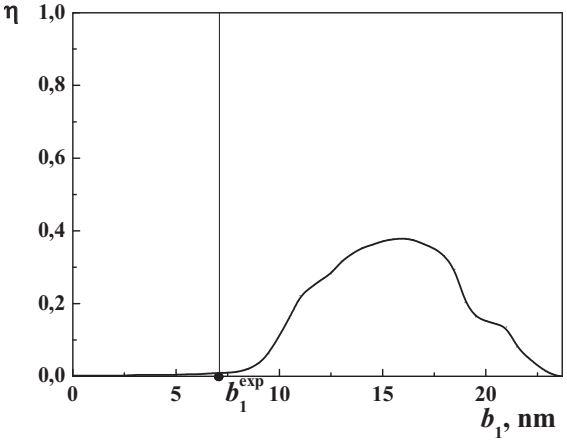

Fig. 4. Dependence of the relative amplification η on the position b_1 of the internal barrier in a common potential well

states are as follows: $\tau_1 = 19.22$ ps, $\tau_2 = 2.20$ ps, and $\tau_3 = 1.89$ ps.

In order to study the contribution of two-photon processes to the formation of the electron active dynamic conductivity in RTSs, the corresponding calculations for laser quantum transitions from the third excited electronic state are carried out in the framework of the one- and two-photon approximations of the theory developed in the previous section. To satisfy the weak-signal conditions $U_1 = e\mathcal{E}_1 z_5 \ll \Omega_1$ and $U_2 = e\mathcal{E}_2 z_5 \ll \Omega_2$, the U_1- and U_2-values are selected to be small: $U_1 = 10^{-3}\Omega_1$ and $U_2 = 10^{-3}\Omega_2$.

The results of calculations of the active dynamic conductivity and its partial components as functions of the internal barrier position b_1 in the common potential well b obtained in the one- and two-photon approximations are shown in Fig. 3. The calculations are carried out for the laser quantum transitions from the third quasi-stationary state that give rise to the emission of one photon with the energy $\Omega_1 = \Omega_{32}$ (transition $3 \to 2$ in the one-photon approximation, the component $\sigma_{32}^{(1)}$, triangles) and two photons with the energies $\Omega_1 = \Omega_{32} = E_3 - E_2$ and $\Omega_2 = \Omega_{21} = E_2 - E_1$ (consecutive transitions $3 \to 2$ and $2 \to 1$ in the two-photon approximation, the components $\sigma_{32,21}^{(II)}$ (circles), $\sigma_{32,21}^{(II)+}$ (solid curve), and $\sigma_{32,21}^{(II)-}$ (dashed curve)). Figure 3 also illustrates the dependences of the conductivity $\sigma_{31}^{(1)}$ in transition $3 \to 1$, which is competing to transition $3 \to 2$, on the parameter b_1 calculated in the one-photon approximation (the dotted curve).

The contribution of two-photon transitions to the total dynamic conductivity in comparison with the one-photon approximation will be characterized by the relative amplification $\eta = (\sigma^{(II)} - \sigma^{(1)})/\sigma^{(II)}$. The dependence $\eta(b_1)$ is shown in Fig. 4. One can see that two intervals of variation can be distinguished for the parameter b_1: 0 nm $\leq b_1 \leq$ 8 nm and 8 nm $\leq b_1 \leq$ 23.8 nm.

The main criterion formulated, while optimizing the performance of the active zone or cascade in QCLs or QCDs, consists in that the dynamic conductivity maximum in the required quantum transition should be realized for a definite QCL or QCD geometrical configuration. As was found in works [5–7], this conductivity is governed by the electron flux at the nanosystem output, and it has to be much higher in comparison with both the conductivity component in the opposite direction and the conductivity values that are formed in other quantum transitions.

In the first interval of b_1-variation, which contains the experimental geometrical configuration b_1^{exp}, the mentioned condition is satisfied, because $\sigma_{32}^{(1)} \approx \approx \sigma_{32}^{(1)+} \gg \sigma_{32}^{(1)-}, \sigma_{31}^{(1)}$. From Fig. 4, it is evident that the contribution of two-photon processes is small ($\eta < 2\%$) in this interval; therefore, no two-photon laser generation takes place. Hence, in the mentioned interval of b_1-variation, the analyzed RTS can effectively operate as an active zone of QCL, in which one-photon laser transitions with the frequency $\Omega = \Omega_{32}$ are realized.

In the second interval of b-variation, the condition for the performance optimization of the active zone of QCL is not obeyed, because (i) if 8 nm $\leq b_1 \leq$ 12 nm, we have $\sigma_{31}^{(1)} \gg \sigma_{32}^{(1)}, \sigma_{32,21}^{(\mathrm{II})}$, i.e. the conductivity formed in transition $3 \to 1$ prevails; (ii) if 12 nm $\leq$ $\leq b_1 \leq$ 14.7 nm, we have $\sigma_{32,21}^{(\mathrm{II})} \approx \sigma_{32,21}^{(\mathrm{II})-} \gg \sigma_{32,21}^{(\mathrm{II})+}$, $\sigma_{31}^{(1)}$, i.e. the conductivity determined by the flux in the opposite direction to the RTS output prevails; (iii) if 14.7 nm $\leq b_1 \leq$ 19.7 nm, we have $\sigma_{31}^{(1)} \gg \sigma_{32}^{(1)}$, $\sigma_{32,21}^{(\mathrm{II})}$, i.e. the conductivity formed in transition $3 \to$ $\to 1$ prevails; and (iv) finally, if 19.7 nm $\leq b_1 \leq$ $\leq$ 23.8 nm, we have $\sigma_{32,21}^{(\mathrm{II})} \approx \sigma_{32,21}^{(\mathrm{II})-} \gg \sigma_{32,21}^{(\mathrm{II})+}, \sigma_{31}^{(1)}$, i.e. the conductivity determined by the flux in the opposite direction to the RTS output prevails.

From Fig. 4, one can see that the dependence $\eta(b_1)$ gradually grows in the interval 8 nm $\leq b_1 \leq$ 16 nm, forms a maximum $\eta \approx 0.38$ at $b_1 \approx$ 16 nm, and afterward gradually vanishes, as $b_1 \to$ 23.8 nm. Hence, by varying b_1, it is possible to obtain such geometrical configurations of examined RTSs, which play the role of an active zone in QCL, when the laser generation can be enhanced up to 38% ($b_1 \approx$ 16 nm, $\sigma_{32,\,21}^{(\mathrm{II})} \gg \sigma_{32}^{(1)}, \sigma_{31}^{(1)}$) owing to two-photon electron transitions. For those RTS configurations, the total conductivity formed in one- and two-photon transitions is determined, to a great extent, by the partial component of the electron flux directed in the opposite direction to the nanostructure output. As one can see from Fig. 2, *b*, the electron lifetimes in the relevant quasi-stationary states become large in the obtained geometrical configurations, which is a substantial negative factor that interferes a correlated coherent electron transport through the active zone and the cascade of QCLs. Therefore, the performance optimization conditions [5–7] are not satisfied for those RTS configurations.

4. Conclusions

On the basis of exact solutions obtained for the full Schrödinger equation in the dipole approximation, a quantum-mechanical theory of active dynamic conductivity in the three-barrier active zone of QCL in a weak electromagnetic field, when one- and two-photon laser generation processes are realized, is developed. The variation in the position of the internal barrier in the common potential of the nanostructure is found to result in such geometrical configurations where the contribution of two-photon radiation processes to the formation of the total dynamic conductivity becomes substantial, amounting to not less than 38%. The calculation of the active dynamic conductivity made it possible to reveal that, for the studied RTS, the processes of two-photon generation manifest themselves in those of its geometrical configurations, in which the total dynamic conductivity is mainly determined by the electron flux in the direction opposite to the nanosystem output. It is established that the conditions of effective one-photon laser generation at the quantum transition between the third and second quasi-stationary electronic states are satisfied in the experimentally analyzed RTS configuration.

The author is sincerely grateful to Head of the Chair of Theoretical Physics of Yu. Fed'kovych National University of Chernivtsi, Dr. Sci. (Phys.-Math.), Professor M.V. Tkach for his useful advice concerning the writing of this work and the discussion of the results obtained.

1. D. Bachmann, M. Rosch, C. Deutsch, M. Krall, G. Scalari, M. Beck, J. Faist, K. Unterrainer, and J. Darmo, Appl. Phys. Lett. **105**, 181118 (2014).
2. J.M. Wolf, A. Bismuto, M. Beck, and J. Faist, Opt. Express **22**, 2111 (2014).
3. A. Buffaz, M. Carras, L. Doyennette, A. Nedelcu, X. Marcadet, and V. Berger, Appl. Phys. Lett. **96**, 172101 (2010).
4. D. Hofstetter, F.R. Giorgetta, E. Baumann, Q. Yang, C. Manz, and K. Kohler, Appl. Phys. Lett. **93**, 221106 (2008).
5. M.V. Tkach, Ju.O. Seti, I. V. Boyko, and O.M. Voitsekhivska, Condens. Matter Phys. **16**, 33701 (2013).
6. M. Tkach, Ju. Seti, I. Boyko, and O. Voitsekhivska, Rom. Rep. Phys. **65**, 1443 (2013).
7. M. Tkach, Ju.O. Seti, V.O. Matiek, and I.V. Boyko, Zh. Fiz. Dosl. **16**, 4701 (2012).
8. E. Saczuk and J.Z. Kaminski, Phys. Status Solidi B **240**, 603 (2003).
9. E. Saczuk and J.Z. Kaminski, Laser Phys. **15**, 1691 (2005).
10. N.V. Tkach and Ju.A. Seti, JETP Lett. **95**, 271 (2012).
11. N.V. Tkach and Ju.A. Seti, Fiz. Tekh. Poluprovodn. **48**, 610 (2014).
12. A.B. Pashkovskii, JETP Lett. **89**, 30 (2009).
13. A.B. Pashkovskii, Fiz. Tekh. Poluprovodn. **45**, 759 (2011).
14. N.V. Tkach and Ju.A. Seti, Low Temp. Phys. **35**, 556 (2009).
15. Y. Ando and T. Itoh, J. Appl. Phys. **61**, 1497 (1987).
16. S. Kumar, C. Wang, I. Chan, Q. Hu, and J.L. Reno, Appl. Phys. Lett. **95**, 141110 (2009).

Received 03.02.15.
Translated from Ukrainian by O.I. Voitenko

І.В. Бойко

ВНЕСОК ДВОФОТОННИХ ЕЛЕКТРОННИХ ПЕРЕХОДІВ У ФОРМУВАННІ АКТИВНОЇ ДИНАМІЧНОЇ ПРОВІДНОСТІ ТРИБАР'ЄРНИХ РЕЗОНАНСНО-ТУНЕЛЬНИХ СТРУКТУР ІЗ ПОСТІЙНИМ ЕЛЕКТРИЧНИМ ПОЛЕМ

Р е з ю м е

У наближенні ефективних мас та прямокутних потенціальних ям і бар'єрів для електрона, з використанням знайдених розв'язків повного рівняння Шредінгера, розвинена теорія активної динамічної провідності трибар'єрної резонансно-тунельної структури з прикладеним постійним поздовжнім електричним полем у слабкому електромагнітному полі з урахуванням внеску лазерних одно- та двофотонних електронних переходів з різними частотами. Показано, що для лазерних електронних переходів величина внеску двофотонних переходів у формуванні загальної величини активної динамічної провідності в лазерних переходах не більша за 38%. Встановлено геометричні конфігурації резонансно-тунельної структури, для яких за рахунок двофотонних лазерних електронних переходів отримується зростання інтенсивності лазерного випромінювання.